Pol. J. Environ. Stud. Vol. 32, No. 1 (2023), 113-124
DOI: *10.15244/pjoes/153022* ONLINE PUBLICATION DATE: 2022-12-05

Original Research

Grain Size Characteristics from Dry Playa Chagan Nur in Northern China

Haonian Li[#], Zhongju Meng[#], Xiaohong Dang, Shuai Qi, Siqin Bao*

College of Desert Control Science and Engineering, Inner Mongolia Agricultural University, Hohhot, P.R. China

Received: 28 June 2022
Accepted: 26 August 2022

Abstract

Dry salt lakes are widely distributed in semi-arid regions. Dry lake beds have been found to have a greater capacity to release dust. However, the particle size characteristics of dry lakebed soils have rarely been studied. To reveal the soil grain size characteristics, we used surface and subsurface soil from dry lake beds in semi-arid regions with different soil crusts as the object of study. We used particle size parameters and class-standard deviation methods to study the particle size variation patterns and the degree of variability. The results show that the dry lake was mainly composed of clay (1.36%-43.96%) and silt (5.5%-67.94%) particles. Soil particle characteristics show the Mean size (Mz) of (0.65-8.89 φ), poorly sorted (0.79-3.38 φ) and a clear linear relationship between dry lake bed skewness and sorting. There is a high variability between soil particle size fractions across the lake bed, with soil crusts and soil moisture protecting the loss of subsurface soil particles, hence the differences between surface and subsurface soil particles. However, the destruction of the soil crust and the evaporation of soil moisture accelerates the wind erosion of the subsurface soil particles. In the dry lake area, vegetation construction has promoted the accumulation of sand content (73.28% -93.08%). We found that the fractions 0.19-9.15 μm, 9.15-36.99 μm, 36.99-366.93 μm, and 366.93-1214.72 μm are susceptible to respond to environmental changes and contribute to dust storms. Therefore, local governments should treat and manage dried-up lakes to reduce the impact of salt dust on the ecosystem.

Keywords: semi-arid dry lake, semi-arid dry lake, Lake Chagan Nur, grain size characteristics, grain size class-standard deviation

Introduction

Large salt lakes account for 44% of the volume and 23% of the area of all lakes on Earth. Most salt lakes are located in inland basins in arid and semi-arid regions and are diverse [1, 2]. They are found in North America [3, 4], the Mexican highlands [5], Iran [6], and northern China [7, 8]. Lakes in arid and semi-arid regions have different hydrology and ecology compared to lakes in humid regions. This determines their sensitivity to climate change and human activity, and they are often affected by riverine, lacustrine and wind processes simultaneously. Lakes in arid and semi-arid regions, as an essential part of the regional water cycle, have evolved over time as a unique sink continuously recharged by surface water and groundwater. However,

# The authors contributed equally to this article.
*e-mail: baosiqin163@163.com

evaporation has exceeded precipitation and inflow in the last decades due to climate change and human activities. Many terminal lakes have undergone dramatic drying, and the Lop Nor on the eastern edge of the Tarim Basin and Lake Aby in China [9, 10], and Lake Hamon in the Sistan Basin of Iran [11, 12] and around the Montero region of northern Spain [13] and the Mojave Desert in the United States [14, 15] have even dried up. When this happens, a playa is created, a dry lake bed in an arid or semi-arid region.

Lake Chagan Nur, a major saltwater lake, is a prime example of the environmental tragedy in northern China, where climatic and anthropogenic changes can be significant. Since the 1960s, the lake's surface area decreased dramatically until 2002, when the western part of Chagan Nur Lake dried up completely [16]. Because of its unique ecosystem and the extent of its deterioration, the fate of Lake Chagan Nur has become an active but controversial research topic in recent years. Various aspects of dried-up lakes, including the leading causes of drying up and the effects of dried-up lake beds on the material cycle of northern Chinese ecosystems under wind-generated environments, have been studied from different perspectives. Mashat [17] and Varga [18] used Total Ozone Mapping Spectrometer (TOMS) satellite images on a global scale and found that dry lake beds are the primary source of dust in the world. Frie [19] and Motaghi [20] analyzed the elemental geochemistry of wind-eroded sediments from dry lake beds using particle-induced X-ray emission. Dried lakes in the arid regions of northwest China have been reported so far as important dust release areas. The sediment and cover of dry lakes influence dust release and wind erosion processes. There is spatial variability in surface soil grain size in the dry lakes [21]. However, research into the grain size characteristics of loose soils in dry lake beds in aeolian environments in semi-arid regions is still unclear. This is very important because particle size analysis can be used to distinguish depositional environments and to identify water or wind conditions that formed the depositional environment [22-24]. They can be used to define the depositional environment based on the frequency of each particle size class in a log-log plot [25] or using a two-dimensional scatter plot by various statistical parameters of the particle size distribution [26]. The statistical distribution of various particle size characteristics (e.g., mean particle size, standard deviation, and kurtosis) also provides a good indicator of how aeolian dynamics control the movement patterns (creep, saltation, and suspension) and the quality of gravel transport [27]. On the other hand, the aeolian process also affects the particle size distribution. Mahiques [28] proposed a method based on this theory, the particle size class-standard deviation method, where the standard deviation is a common indicator of trends in data dispersion. The larger the standard deviation, the higher the degree of individual variability and vice versa, so the method easily identifies particle size intervals with the highest variability along the depositional sequence. This method is more meaningful for spatial size classification analysis than individual size values, so identifying potential size fractions is key to size classification analysis. The method has been successfully applied to studying marine sediments [28-30]. However, the method has been applied less frequently in wind deposition studies. Guan [31] and Wang [32] used this method in a useful attempt on loess deposits and found it applicable for such purposes as well.

This study investigated the soil particle size distribution in the dry lake bed of Chagan Nur in northern China. The objectives of this study were (1) to characterize the distribution of soil particles in the study area and (2) to discuss the regional particle size characteristics and spatial variability in terms of soil particle size distribution. To provide a theoretical basis for the ecological restoration of the dried-up lake bed area.

Material and Methods

Study Area

Chagan Nur Lake is located in northern China. The dry lake area in the south of the Otindag sandy land, the north is a typical grassland area, between 114°45′E and 115°04′E and between N43°22′N and 43°29′N. Chagan Nur Lake is divided into two regions, east and west, the recharge of the lake are mainly affected by some rivers originating from the Otindag sandy land, where the Gogsdai River is injected into the East Lake from east to west. The Nuggs River flows into the large lake on the west side from the southwest, there is a dike between the two lakes, and there is a sluice gate to control the flow of water from the East Lake to the West Lake (Fig. 1). In recent years due to climate drought, vegetation degradation and overload grazing, and other natural and human economic activities, the water surface of the big lake of Chagan Nur has been shrinking year by year. In the past nearly four decades, the lake area has decreased by about 75 km^2, about to -18.3 km^2 /decade, and in 2002 there was a sudden change event, the lake area from 74.8 km^2 in 2001 to 28.5 km^2 in 2002, at a rate of 46.3 km^2/a, while the West Lake dried up completely [33]. The area belongs to the middle temperate semi-arid continental monsoon climate zone, with frequent droughts and high winds in spring, mild and rainy in summer under the influence of southeast monsoon, and dry and cold in winter under the control of Mongolian high pressure, with its annual average temperature of 0.6ºC, minimum temperature of -42.4ºC and maximum temperature of 39.1ºC, annual average precipitation in between 240-260 mm, mostly concentrated in July and August each year; the average annual evaporation is 1956 mm; the average wind speed is 3.5 m/s.

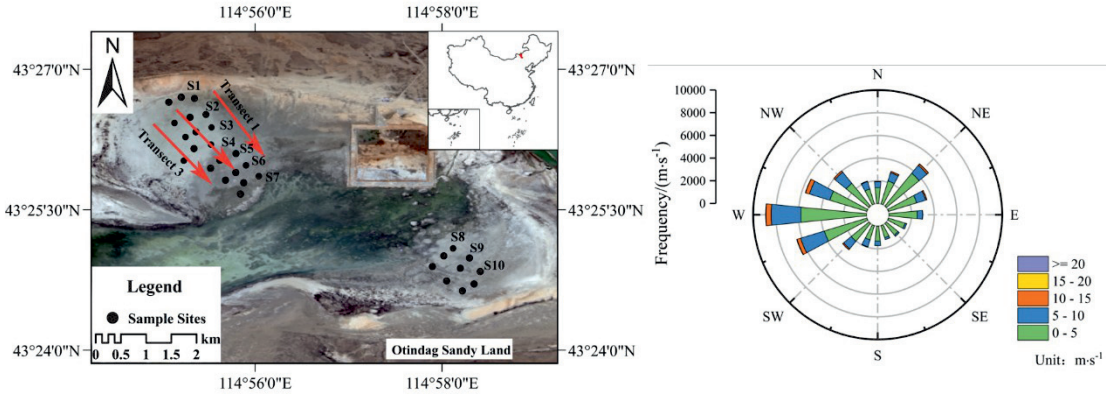

Fig. 1. Distribution of sampling points and wind direction wind frequency rose map of Lake Chagan Nur.

Soil Sampling and Data Analysis

Through the preliminary survey of the dry lake bed from northwest to southeast, based on the surface vegetation type and soil crust morphology (Fig. 2), we divided 10 sample site types, from northwest to southeast, in the order of S1 to S10. These ten sample site types are representative of all surface conditions in this dry lake area. Spatial variation in aeolian conditions and construct vegetation produced these ten sample site types from the lake centre to the lakeshore. We collected soils in the spring of 2021 in the dry lake bed of Chagan Nur along transect 2 (Fig. 1), and each type of sample site was selected in eastward (transect 1) and westward (transect 3). And a total of 30 sampling sites were selected for the entire dry lake bed, and surface (0-3 cm) and subsurface (3-10 cm) layers were collected at each sample site, with a collection area of 20 cm × 20 cm. A total of 60 soil samples were collected. After removing plant roots and residues, each sample weighed 200 g. Soil moisture was measured at each sampling site, and the latitude and longitude of each sampling site were recorded (Table 1).

We measured the particle size distribution of soil samples using an Analysette 22 NanoTec laser particle size meter (FRITSCH, Germany). Measurement range 0.01 to 2000 µm, accuracy better than 0.6%, accuracy/reproducibility better than 0.5% variable. The soil samples were treated with organic matter removal and desalination prior to measurement. We used the USDA sediment size classification criteria, and in the calculations, particle size was measured using φ (U), using the Udden - Wenworth particle size scale, transformed according to Kum-dein's algorithm to calculate ($\varphi = -log_2 d$, where d is the size in millimeters) [34]. The mean size (Mz), sorting (Sd), skewness (Sk), and kurtosis (Kg) were also calculated according to the equations devised by [39].

$$Mz = \frac{1}{3}(\varphi 16 + \varphi 50 + \varphi 84) \quad (1)$$

$$Sd = \frac{\varphi_{84} - \varphi_{16}}{4} + \frac{\varphi_{95} - \varphi_5}{6.6} \quad (2)$$

$$SK_1 = \frac{\varphi_{84} + \varphi_{16} - 2 \times \varphi_{50}}{2 \times (\varphi_{84} - \varphi_{16})} + \frac{\varphi_{95} + \varphi_5 - 2 \times \varphi_{50}}{2 \times (\varphi_{95} - \varphi_5)} \quad (3)$$

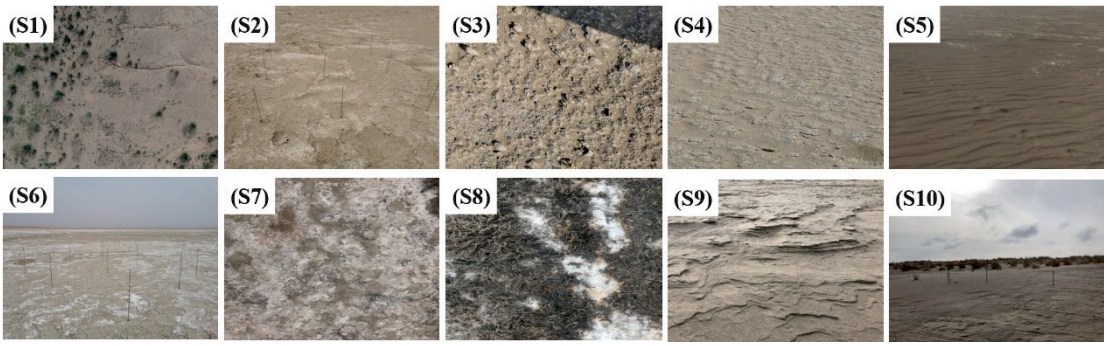

Fig. 2. Typical soil for the 30 sampling points shown in Fig. 1: the sampling points extend the transect from northwest to southeast in the order S1 to S10. S1 corresponds to the lakeshore zone and has the distribution of *Achnatherum splendens*. S2 corresponds to the fluffy crust. S3 corresponds to crusts, where the uneven crust intercepts some of the wind eroded particles. S4 corresponds to the gradual breaking of the crust by the collision of wind eroded particles. S5 corresponds to the salt soil that can move with the wind. S6, S7 correspond to the salt-covered crust and have different crushing states. S8 corresponds to a loose salt soil with *Suaeda glauca* distribution. S9 corresponds to sand crust. S10 corresponds to the sand.

Table1. location and general characteristics of sampling point.

Sampling sites	Vegetation type	Soil moisture content/%	
		Surface	Subsurface
S1	*Achnatherum splendens*	4%	9%
S2	None	4%	9%
S3	None	6%	27%
S4	None	7%	29%
S5	None	10%	27%
S6	None	20%	30%
S7	None	12%	18%
S8	*Suaeda glauca*	3%	34%
S9	None	4%	13%
S10	None	5%	6%

$$Kg = \frac{\varphi_{95} - \varphi_5}{2.44 \times (\varphi_{75} - \varphi_{25})} \quad (4)$$

The standard deviations for all samples in both splines were calculated based on the obtained soil particle size. The particle size standard deviation algorithm is the most commonly used method for extracting sensitive particle size fractions from wind-formed sediment. The principle is to obtain the number and distribution range of the particle size fraction by studying the standard deviation of the volume content of each particle size level given by the laser particle size analysis. A high standard deviation value reflects a large variation in the volume content of different samples in a certain size range, while a low standard deviation reflects a small variation in a certain size range [31].

Results

General Particle Size Composition and Distribution

Table 2, Table A1, and Fig.3 summarize the particle size composition and parameters of our samples from the dried lake in Chagan Nur. Overall, the MZ of the soil ranged from 0.65 φ to 8.90 φ with a mean of 5.62±2.77 φ. The standard deviation ranged from 0.74 φ to 3.72 φ with a mean of 2.25±0.79 φ. The Sk ranged from - 0.57 to 0.82 with a mean of -0.09±0.39 φ. The Kg ranged from 0.61 to 3.62 with a mean of 1.25±0.61. Silt account for more than 40% of the total volume of all particle sizes, followed by clay with 22%, fine sands with 11%, medium sands with 12%, coarse sands with 10%, and very fine and very coarse sands with less than 2%.

Grain size in the surface (0-3 cm layer) of the dry lake bed is coarser than the subsurface (3-10 cm layer), with silt accounting for 38% of the total volume, followed by 23% of clay, 14% of medium sands, 10% of fine and coarse sands, and 2% of very fine and very coarse sands. It is more obvious that the particle size distribution shows a trend of becoming finer from the surface (0-3 cm layer) to subsurface (3-10 cm layer) at sample points S1 to S7 but shows a trend of becoming coarser at sample points S8 to S9. The Mz of the surface layer of the dry lake bed ranged from 1.32 φ to 3.72 φ with a mean value of 2.43±0.67 φ, and the standard deviation of the subsurface soil ranged from 0.74 φ to 3.38 φ with a mean value of 2.08±0.87 φ (Fig. 3). From S1 to S8, it showed that the Mz of the subsurface layer (1.04 φ to 8.32 φ) was larger than that of the surface layer (0.88 φ to 8.56 φ), and the Mz (S1 position) at the edge of the dry lake bed varies widely. However, the wind erosion and wind accumulation conversion phenomenon occurred at the S9 and S10 locations, and the Mz increases from the subsurface to the surface layer, and the Mz increases from 0.72 φ and 1.55 φ to 3.30 φ and 4.84 φ. The standard deviation of the dry lake bed surface layer ranged from 1.47 φ to 3.25 φ with a mean value of 2.43±0.67 φ, and the standard deviation of the subsurface ranged from 0.77 φ to 3.08 φ with a mean value of 2.08±0.87 φ.

Soil particle size in the dry lake area was mostly poorly sorted (Fig. 3). The Sk shows that the range of the soil surface layer -0.53 to 0.82, from S2 to S7, is mostly extremely negatively skewed, and S8 to S10 shows extremely positive-skewed. In the soil subsurface layer -0.50 to 0.27, from S2 to S7, is mostly very negative-skewed, and S8 to S10 shows very positive-skewed. The Kg is between 0.69 and 3.46 at the sediment surface layer, S1 to S7 is almost a Mesokurtic distribution, while S8 is very sharp and narrow kurtosis, and even S9 has an extremely leptokurtic distribution (Fig. 3). Compared with the surface layer, the subsurface kurtosis mostly shows a leptokurtic distribution.

Table 2. Particle size of soil of Chagan Nur Lake.

Position	0-3 cm			3-10 cm			0-10 cm		
	Clay	Silt	Sand	Clay	Silt	Sand	Clay	Silt	Sand
S1	7.33 ± 0.29A	19.40 ± 0.70B	73.28 ± 0.44A	28.99 ± 2.56A	57.90 ± 2.00A	13.11 ± 0.91C	18.86 ± 10.98A	38.65 ± 19.31A	43.20 ± 30.09A
S2	26.53 ± 3.88A	55.57 ± 8.31A	17.90 ± 4.82B	28.34 ± 4.48A	55.16 ± 6.16A	22.82 ± 6.58C	27.44 ± 4.28A	55.36 ± 7.32A	17.20 ± 4.08A
S3	27.72 ± 1.74A	61.45 ± 8.84A	10.83 ± 7.59B	25.17 ± 1.03A	52.05 ± 7.43A	22.82 ± 6.58C	26.44 ± 1.92A	56.75 ± 9.42A	16.82 ± 9.29A
S4	32.53 ± 1.50A	57.54 ± 8.19A	9.93 ± 6.70B	36.75 ± 4.40A	61.23 ± 6.44A	5.17 ± 3.49C	34.64 ± 3.91A	59.39 ± 7.59A	5.97 ± 6.39A
S5	43.96 ± 5.13A	56.04 ± 5.13A	0.00 ± 0.00	35.09 ± 2.55A	59.74 ± 6.04A	5.17 ± 3.49C	39.52 ± 6.01A	57.89 ± 5.90A	2.59 ± 3.58A
S6	28.18 ± 1.70A	51.53 ± 6.61A	20.29 ± 7.58B	27.34 ± 1.19A	53.19 ± 5.21A	19.46 ± 5.53C	27.76 ± 1.53A	52.36 ± 6.01A	19.88 ± 6.65A
S7	24.78 ± 3.73A	67.94 ± 4.45A	7.28 ± 0.072B	26.59 ± 1.74A	57.58 ± 5.63A	15.83 ± 5.46C	25.68 ± 3.05A	62.76 ± 7.25A	11.56 ± 5.78A
S8	1.36 ± 0.22A	5.55 ± 0.30D	93.08 ± 0.14A	0.50 ± 0.10B	1.29 ± 0.12A	98.18 ± 0.25A	0.93 ± 0.46A	3.42 ± 2.14A	95.63 ± 2.56A
S9	4.69 ± 1.66A	12.50 ± 0.64C	82.81 ± 1.71A	0.88 ± 0.12B	2.43 ± 0.05B	96.59 ± 0.15B	2.78 ± 2.24A	7.46 ± 5.05A	89.70 ± 6.99A
S10	10.64 ± 0.84A	39.88 ± 1.83A	49.46 ± 1.08B	1.32 ± 0.11B	3.40 ± 0.45A	95.19 ± 0.55B	5.98 ± 4.70A	21.64 ± 18.29A	72.33 ± 22.88A

Note: Different uppercase letters indicate significant differences ($p<0.05$, Games- Howell test) between different sample sites. S1 to S10 represent the dry lake bed from northwest to southeast, respectively. S1 corresponds to the lakeshore zone and has the distribution of *Achnatherum splendens*. S2 corresponds to the fluffy crust. S3 corresponds to crusts, where the uneven crust intercepts some of the wind eroded particles. S4 corresponds to the gradual breaking of the crust by the collision of wind eroded particles. S5 corresponds to the salt soil that can move with the wind. S6, S7 correspond to the salt-covered crust and have different crushing states. S8 corresponds to a loose salt soil with *Suaeda glauca* distribution. S9 corresponds to sand crust. S10 corresponds to the sand.

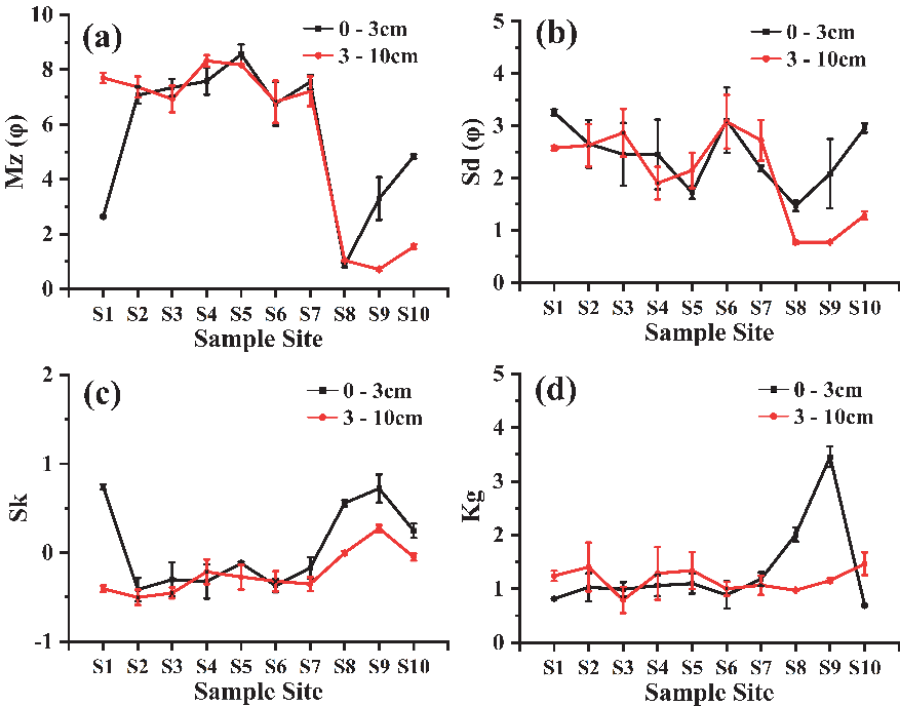

Fig. 3. Grain size composition and characteristics (Mz, mean grain size; Sd, standard deviation; Sk, skewness; Kg, kurtosis) for the sampling point in Chagan Nur Lake region. S1 to S10 represent the dried lake bed from northwest to southeast, respective.

Table A1. Proportion (%) of soil particle distribution at different locations in the dry lake bed.

Soil particle size content	Surface (0 -3 cm)									
	S1	S2	S3	S4	S5	S6	S7	S8	S9	S10
Clay	7.33±0.29A	26.53±3.88A	27.72±1.74A	32.53±1.50A	43.96±5.13A	28.18±1.70A	24.78±3.73A	1.36±0.22A	4.69±1.66A	10.64±0.84A
Silt	19.40±0.70B	55.57±8.31A	61.45±8.84A	57.54±8.19A	56.04±5.13A	51.53±6.61A	67.94±4.45A	5.55±0.30D	12.50±0.64C	39.88±1.83A
Very fine sand	2.69±0.22A	2.02±1.20A	0.23±0.10A	0.42±0.39A	0.00±0.00	1.18±0.48A	0.07±0.09A	1.99±0.10A	0.56±0.05A	6.56±0.04B
Fine sand	4.04±0.39C	11.79±0.68C	2.74±1.94C	4.27±2.44C	0.00±0.00	7.91±3.76C	6.65±0.86C	8.62±0.75C	61.66±0.07A	26.32±0.39B
Medium sand	17.45±1.03A	4.09±3.93A	7.78±5.50A	5.24±3.88A	0.00±0.00	6.10±1.52A	0.56±0.41A	23.70±1.28A	20.60±1.72A	13.01±1.88A
coarse	37.31±0.76B	0.00±0.00	0.07±0.10B	0.00±0.00	0.00±0.00	5.11±7.22B	0.00±0.00	50.19±0.65A	0.00±0.00	3.19±1.87B
Very coarse	11.79±1.51A	0.00±0.00	0.00±0.00	0.00±0.00	0.00±0.00	0.00±0.00	0.00±0.00	8.57±2.62A	0.00±0.00	0.38±0.41B

Note: The values in the table are means ± SD (n = 3). Different uppercase letters indicate significant differences ($p < 0.05$, Games- Howell test) between different sample sites. S1 to S10 represent the dry lake bed from northwest to southeast, respectively. S1 corresponds to the lakeshore zone and has the distribution of *Achnatherum splendens*. S2 corresponds to the fluffy crust. S3 corresponds to crusts, where the uneven crust intercepts some of the wind eroded particles. S4 corresponds to the gradual breaking of the crust by the collision of wind eroded particles. S5 corresponds to the salt soil that can move with the wind. S6, S7 correspond to the salt-covered crust and have different crushing states. S8 corresponds to a loose salt soil with *Suaeda glauca* distribution. S9 corresponds to sand crust. S10 corresponds to the sand.

	Subsurface (3 - 10cm)									
	S1	S2	S3	S4	S5	S6	S7	S8	S9	S10
Clay	28.99±2.56A	28.34±4.48A	25.17±1.03A	36.75±4.40A	35.09±2.55A	27.34±1.19A	26.59±1.74A	0.50±0.10B	0.88±0.12B	1.32±0.11B
Silt	57.90±2.00A	55.16±6.16A	52.05±7.43A	61.23±6.44A	59.74±6.04A	53.19±5.21A	57.58±5.63A	1.29±0.12B	2.43±0.05A	3.40±0.45A
Very fine sand	0.01±0.02C	1.83±1.71A	2.08±0.70A	0.00±0.00	0.00±0.00	1.41±0.41A	1.25±1.00A	0.56±0.02A	0.33±0.02B	2.88±0.11A
Fine sand	0.02±0.03B	10.23±0.81A	13.29±3.03A	0.83±0.91B	3.47±2.06B	4.55±0.35B	11.29±3.82A	7.78±0.13A	3.74±0.10B	28.70±1.25A
Medium sand	8.83±0.95B	3.74±2.78B	7.38±3.98B	1.19±1.43B	1.70±1.55B	13.46±5.14B	3.30±0.88B	42.84±0.50A	24.25±1.59B	40.48±1.40A
coarse	4.25±1.71D	0.70±0.99E	0.07±0.09E	0.00±0.00	0.00±0.00	0.04±0.04E	0.00±0.00	38.60±1.23B	54.17±0.72A	12.28±1.20C
Very coarse	0.00±0.00	0.00±0.00	0.00±0.00	0.00±0.00	0.00±0.00	0.00±0.00	0.00±0.00	8.41±1.60B	14.10±2.28A	10.85±1.61AB

Note: The values in the table are means ± SD (n = 3). Different uppercase letters indicate significant differences ($p < 0.05$, Games- Howell test) between different sample sites. S1 to S10 represent the dry lake bed from northwest to southeast, respectively. S1 corresponds to the lakeshore zone and has the distribution of *Achnatherum splendens*. S2 corresponds to the fluffy crust. S3 corresponds to crusts, where the uneven crust intercepts some of the wind eroded particles. S4 corresponds to the gradual breaking of the crust by the collision of wind eroded particles. S5 corresponds to the salt soil that can move with the wind. S6, S7 correspond to the salt-covered crust and have different crushing states. S8 corresponds to a loose salt soil with *Suaeda glauca* distribution. S9 corresponds to sand crust. S10 corresponds to the sand.

The surface and subsurface layers of lacustrine sediments in the dry lake bed show a multi-modal distribution due to their complex depositional environment, with peaks in clay, silt, and medium and coarse sands.

Spatial Distribution of Particle Size

Table 2 shows the particle size distribution of the sediment surface and subsurface layers in the dried lake bed. Samples S1 to S10 were selected along the sampling line to characterize the sand particle size.

The particle size distribution of the samples along with S1 to S10 is shown in (Fig. 4). For subsurface soil, 85% of particles at 4.32 φ and 14.47 φ (from 49.90 to 0.04 μm) at S1 to S7, while 95% of the particles were between -1φ and 2.02 φ (from 246.20 to 2000 μm) at S8 to S10, with the S8 to S10 samples showing mainly a single-peaked distribution, suggesting that a single transport or deposition process promoted particle separation. The peaks of the frequency curves for S1, S8, and S9 are significantly higher than the others. The surface sediment samples are single- or four-peaked distributions, showing a narrower distribution and lower

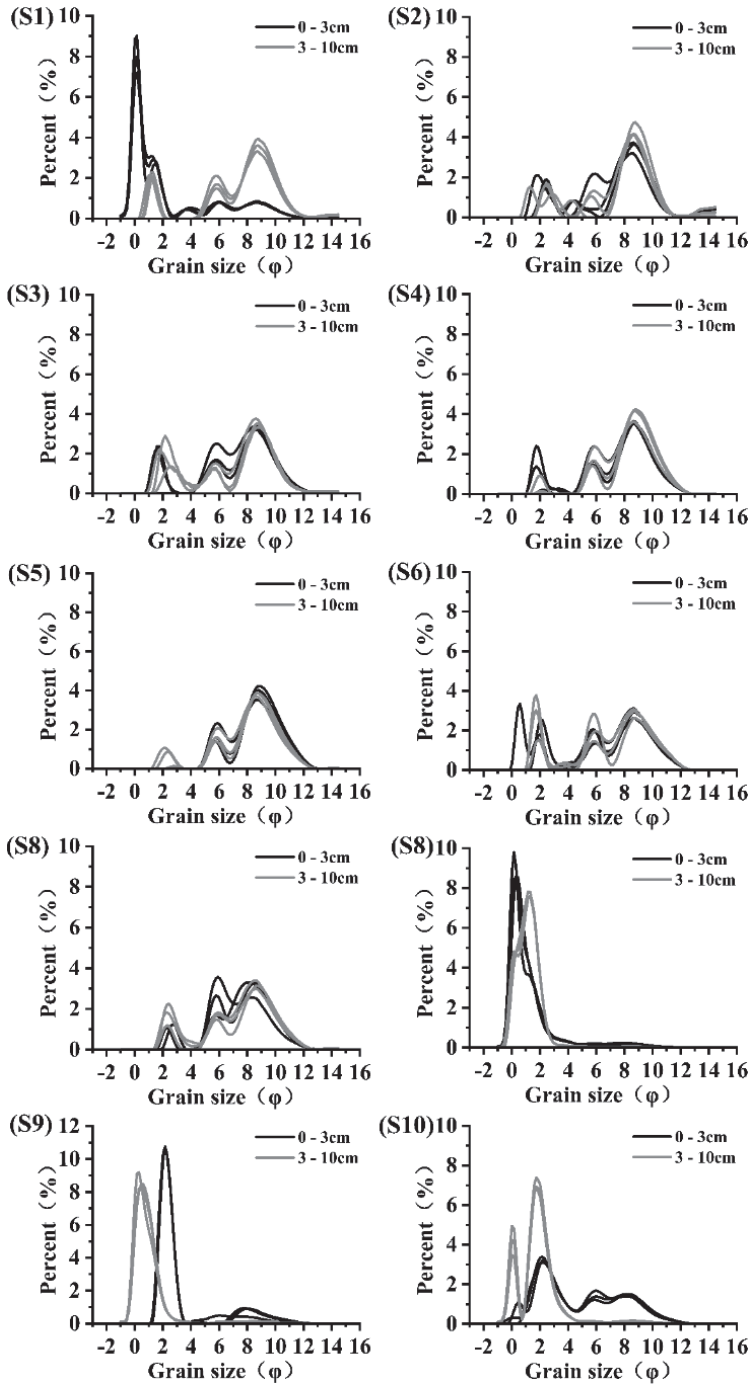

Fig. 4. The particle size distribution and mean frequency distribution of the investigated Chagan Nur Lake.

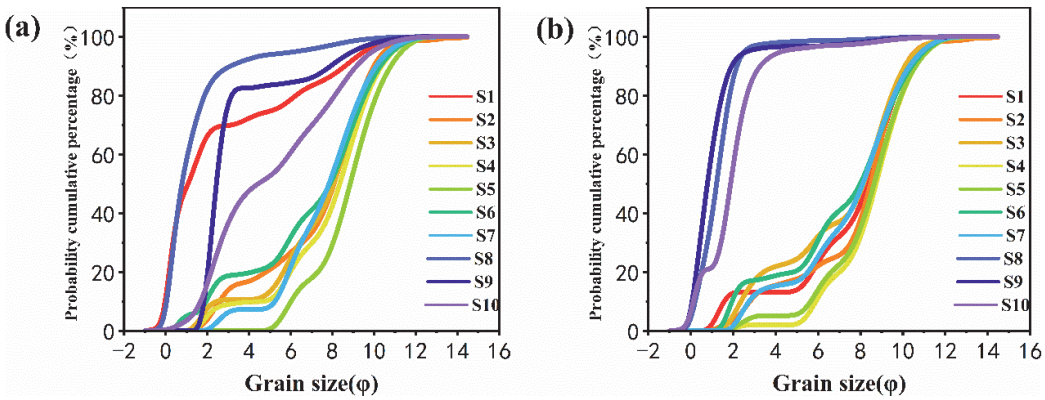

Fig. 5. Logarithmic cumulative probability distribution of soil in the surface (0-3 cm layers) a) and subsurface (3-10 cm layers) b) on the dry lake bed of Chagan Nur Lake.

peaks along with S1 to S10 (Fig. 4), with distributions exhibiting a wide to narrow to a wide range, reflecting the high variability of sediment conditions and poor sort.

Overall, the clay, fine, and very coarse sands contents vary widely from S1 to S10. In particular, the soil particles vary even more from the dry lakeshore to the centre of the lake. Under the effect of wind sorting, clay particles increased from 7.33% to 26.53%, silt particles increased from 19.40% to 55.57%, medium sands decreased from 17.45% to 4.09%, coarse sand decreased from 37.31% to 0%, the Mz became finer, from 2.64φ to 7.06φ, skewness decreased from 0.74 to -0.42, and kurtosis increased from 0.82 to 1.02. From S2 to S7, the clay particles in the dry lake bed exposed on the surface increased from between 24.78% and 43.96%, and between 50.31% and 67.94% for silt content.

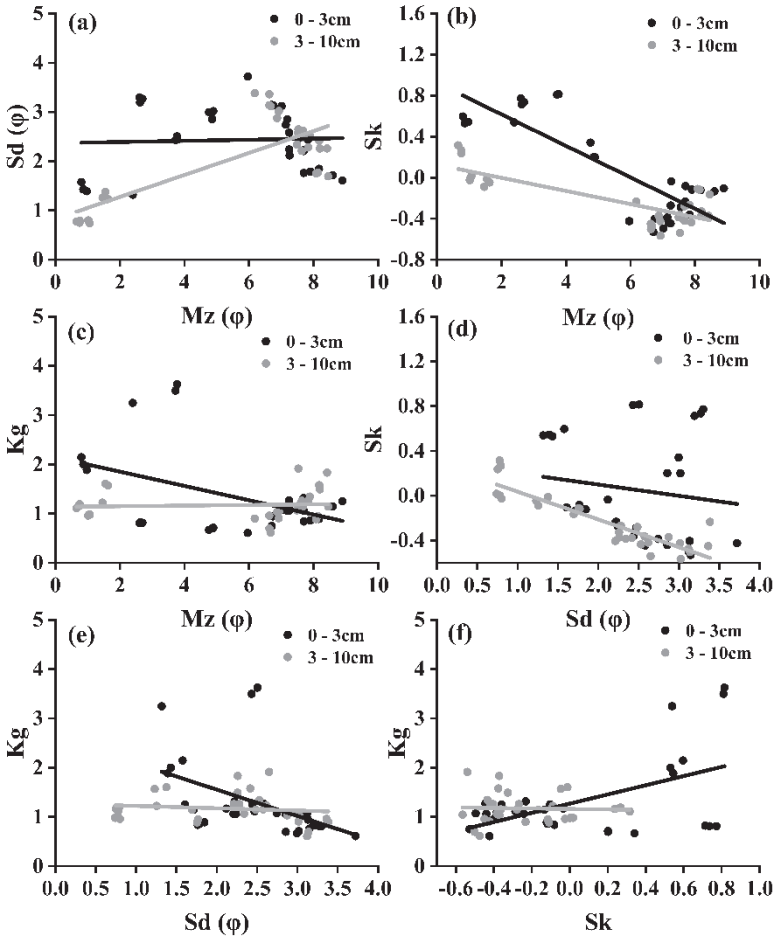

Fig. 6. Bivariate plots of grain size and sorting parameters for soil.

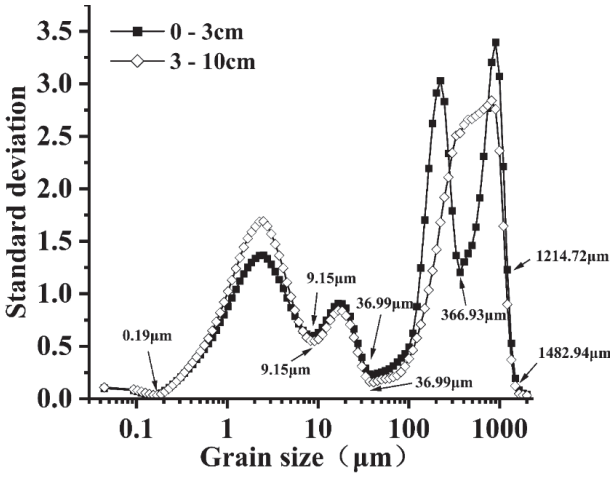

Fig. 7. Standard deviation of particle size classes for the Chagan Nur Lake area.

From the centre of the dry lake to the south-eastern shore of the dry lake, the particle size tends to be refined (Fig. 3). The Mz increases from 0.88 φ to 4.84 φ, the Sd increases from 1.47 φ to 2.96 φ. Clay particles increase from 1.21% to 10.64%, silt particles increase from 5.55% to 39.88%, and coarse and very coarse sands increase from 58.76% to 3.57%. The kurtosis changes from a very sharp and narrow distribution to wide and flat distribution.

With the improvement of sorting, the sands gradually become a symmetrical distribution (Fig. 6d), and there is an obvious relationship between skewness and standard deviation (Fig. 6b). Due to the presence of crusts, the subsurface soil particles tend to become finer with improved sorting (Fig. 6a), and the sand gradually was symmetrically distributed. This suggests that sorting improves when both relatively coarse and fine sand particles are lost, while the presence of physical crusts makes sort poorly.

Standard Deviation of Soil Particle Size

The standard deviation values of the surface layer are larger than those of the subsurface layer, and the shape of the curves and the number of sensitive grain size components in the two sample bands show very good agreement (Fig. 7). Except for (300-737 μm), which defines the limits of the class named in the Wentworth scale according to the size range [34]. This particle size composition belongs to the sand component because fine particles accumulate in the surface layer at S8 and S9. There are four distinct peaks on the standard deviation curve of the soil surface size class corresponding to the size ranges 0.19-9.15 μm, 9.15-36.99 μm, 36.99-366.93 μm, and 366.93-1214.72 μm (Fig. 7). The particle size compositions belonged to the clay-grain component, clay-silt-grain component, silt-sand component, and sand component. And there are three distinct peaks in the soil subsurface layer corresponding to 0.19-9.15 μm, 9.15-36.99 μm, 36.99-366.93 μm, and 366.93-1482.94 μm. The sand component (36.99 to 1482.94 μm) was the component with the highest standard deviation value and the highest sensitivity in the surface and subsurface layers of the soil.

Discussion

Lake Chagan Nur has a temperate semi-arid continental climate, and the wind is the most important transporting force in the region. The area is clay-rich lacustrine sediments, so the entire dry lake bed area S1 to S10 has high clay and slit content, high Mz values, and is poorly sorted. There is a significant variation in surface and subsurface soil particle size. In semi-arid regions, physical soil crust is often the result of rainfall interacting with fine particle such as clay in the surface soil, especially in the presence of large amounts of soluble salts [36]. These crusts form a strong, dense layer that protects the fine particle below from wind erosion and stabilizes the surface [37]. The presence of soil crusts protects the subsurface soil particles from erosion. As a result, the subsurface layer has a finer soil particle content compared to the surface layer. The entire dry lake bed lacked vegetation protection and was artificially planted with *Achnatherum splendens* and *Suaeda glauca* only at S1 and S8. The plants reduced the wind speed and soil erodibility near the surface and increased the retention capacity of wind erosion materials [38, 39]. Vegetation is as one of the most active factors affecting surface wind erosion and will protect the covered part of the surface from wind action. Soil particles are a coarse graining phenomenon at S1, where wind erosion increases the sand content of soil particles and the loss is of clay and silt particles. In particular, there is a greater variation in soil particles from the dry lakeshore to the center of the lake. From S2 to S7, the surface and subsurface soil particle size composition is dominated by clay and silt particles due to the lack of vegetation protection of the surface. Because of the precipitation and strong evaporation capacity in semi-arid regions, physical crusts are formed at the surface, and the formation of physical crusts protects the very fine, fine, and medium sand components of the surface soil. Physical crusts break up in a aeolian environment (Fig. 2, S5), and the S5 surface layer of soil has only clay and silt components and is better sorted than the subsurface layer. From S8 to S10 under the interaction of wind erosion and water erosion, the fine particles are transported from S8 to S10 with the surface sediment, while the coarse particles are mostly intercepted by the action of *Suaeda glauca* to stay in S8. The content of clay and silt particles in the surface soil increased from S8 to S10, and the soil particle size gradually became finer. The study area is in a low-lying playa, which is prone to runoff and ponding of water at the surface after precipitation. The combined effect of wind erosion

and water erosion causes soil particles to show multi-modal migration, so that the distribution of soil particles from S1 to S10 has a multi-peaked distribution. Soil particle size composition analysis and sensitive particle size component analysis, of which were combined to analyze some components of the soil particle composition in the entire dry lake bed at different levels of loss and accumulation. Pye [40] argued that particles <400 μm in size are highly susceptible to wind erosion, and Pye [41] concluded that saltation account for a large proportion of the wind-sand flow and is distributed between 70 and 500 μm, with the fraction of particles <70 μm being transported mainly as suspension. Of the four sensitive fractions (Fig. 7), the 9.15 -36.99 μm fraction is less sensitive and belongs to the clay and silt fraction, and he and the 0.19-9.15 μm fraction are mainly transported in suspension in the overhead airflow. The 36.99-366.93 μm fraction (which belongs to the silt and sand fraction) is mainly transported in short-term suspension near the surface and in hopping or modified hopping mode [42]. The 366.93-1214.72 μm fraction (which is a sand component) has a higher sensitivity compared to the first three components, and its coarse grains are likely from near-source deserts and Wu [43] suggests that sands with grain sizes between 500 and 2000 μm are prone to creep. Pye [40] suggested that during a typical dust storm event, the coarse sand component of sand and silt with a particle size between 70 and 500 μm can only be lifted between a few centimeters and a few meters above the Earth's surface and can be transported horizontally for the same distance. The silt component between 20 and 70 meters is mainly suspended for short distances. It is suspended a few hundred meters above the Earth's surface and transported over distances of up to about 1000 km, mainly at the base of the troposphere. Particles below a few microns can be lifted to heights up to a few kilometers, but are transported over long distances. Dust emissions are usually caused by strong winds acting on dry, fine, and loose soil surface materials and are related to the proportion of mulch as erodible particles and the fine particle content of the surface material [44-47]. In this study, the soil water content increased and then decreased from S1 to S10, and the difference in water content between the surface layer (0-3 cm soil layer) and the subsurface layer (3-10 cm soil layer) was large. The subsurface soil water content inhibits the movement of soil particles, the surface soil inhibits the evaporation of the subsurface soil water content, and there is a greater possibility of soil particle transport throughout the dried lake bed edge compared to the center [48]. Significant differences in the erodible fraction of the soil in the playa surface and agricultural land studied by Alizadeh suggest that the type of dry lake surface is a major factor in sensitivity to wind erosion [20].

Dust storms are usually produced by strong winds acting on dry, loose soil surfaces. Currently, the exposed dry lake bed has an abundance of clay and the formation of hard clay crusts on the clay surface, making the playa surface stable to wind erosion, but there are still areas where the soil surface has been damaged by wind. Due to their high content of fine particles, fragile crusts, and exposed soil surfaces, they are more susceptible to wind erosion. Researchers have made some positive progress in controlling of desertification, with much of the work taking place in areas of fragile ecological conditions and high human activity [49]. Several scholars working on aeolian research have successively proposed ecological and engineering interventions, such as artificial vegetation and checkerboard barriers, to control these desertification hazards in northern China [50].

Conclusion

Particle size analysis is an important tool for differentiating sedimentary environments, providing clues to the characteristics of the aeolian environment at the regional and local scales of dry lakes in semi-arid regions. The soil particles of the dry lake consist mainly of clay and silt particles (4.32-14.47 φ). There were significant differences in soil particle content between the surface and subsurface layers in the soil samples we collected, with the subsurface layer having a finer particle size than the surface layer. The soil particles in the dry lake bed are poorly sorted, the Mean size (Mz) (0.66-8.89 φ) is getting finer and roughly exhibits a negative or very positive skew distribution. There is spatial heterogeneity in the soil particle composition of the dried lake, and the cultivation of *Achnatherum splendens* and *Suaeda glauca* has coarsened the surface soil particles. From the dry lakeshore to the centre of the lake there is a gradual increase in clay and silt particles, the formation of physical crusts and the higher soil water content protects against the loss of subsurface soil particles. The conditions of deposition of soil grain size, subject to the combined effects of wind and water erosion, are very complex and variable. We analyzed the soil particle composition and extracted the sensitive particle size fractions of this habitat and found that 0.19-9.15 μm, 9.15-36.99 μm, 36.99-366.93 μm, and 366.93-1214.72 μm have high sensitivity. These fractions on the dry lake bed are susceptible to respond to environmental changes, and these fractions move in different ways to contribute to dust storms.

Author Contributions

Writing - original draft H. L.; investigation H. L. and S. Q.; methodology, H. L.; formal analysis, S. Q.; data curation, Z.M., X. D.; writing - review and editing, Z.M., X. D. and S. B.; supervision, Z. M. All authors have read and agreed to the published version of the manuscript.

Acknowledgment: We are grateful to the editor for his ability to work on this manuscript during his busy schedule.

Declaration of Interest Statement

The authors declare that they have no known competing financial interests or personal relationships that could have appeared to influence the work reported in this paper.

Funding Acknowledgment Statement

Supported by the Natural Science Foundation of China, No. 42067015. Natural Science Foundation of Inner Mongolia Region, No.2020MS03038 and Basic Research Funds for Universities-Innovation Team Buildin – Desert Ecosystem Protection and Restoration Innovation Team.

Data Availability

The datasets generated during and/or analysed during the current study are available from the corresponding author on reasonable request.

Reference

1. MERNAGH T.P., BASTRAKOV E.N., JAIRETH S., CARITAT P.DE., ENGLISH P.M., CLARKE J.D.A. A review of Australian salt lakes and associated mineral systems. Australian Journal of Earth Sciences, **63**, 131, **2016**.
2. WURTSBAUGH W.A., MILLER C., NULL S.E., DEROSE R.J., WILCOCK P., HAHNENBERGER M., HOWE F., MOORE J. Decline of the world's saline lakes. Nature Geoscience, **10**, 816, **2017**.
3. COLLINS J.D., GILL T.E., LANGFORD R. Characterizing formation processes of Rimrock Lake, a Late Pleistocene-Holocene playa, Harney Basin, south-eastern Oregon, USA, using an end-member mixing analysis. Journal of Quaternary Science, **33**, 721, **2018**.
4. BOWEN M.W., JOHNSON W.C. Holocene records of environmental change in High Plains playa wetlands, Kansas, US. The Holocene, **25**, 1838, **2015**.
5. CALDERÓN-ARREOLA J.B., ALCOCER J., OSEGUERA L.A. A Note of a Unique Inland, Saline Water Fishery: Brine Flies (Diptera: Ephydridae) of Lake Cuitzeo, Mexico. Water, **14**, **2022**.
6. ZIYAEE A., KARIMI A., HIRMAS D.R., KEHL M., LAKZIAN A., KHADEMI H., MECHEM D.B. Spatial and temporal variations of airborne dust fallout in Khorasan Razavi Province, Northeastern Iran. Geoderma, **326**, 42, **2018**.
7. CHEN J., HUANG Q., LIN Y., FANG Y., QIAN H., LIU R., MA H. Hydrogeochemical Characteristics and Quality Assessment of Groundwater in an Irrigated Region, Northwest China. Water, **11**, **2019**.
8. TAO S., FANG J., MA S., CAI Q., XIONG X., TIAN D., ZHAO X., FANG L., ZHANG H., ZHU J., ZHAO S. Changes in China's lakes: climate and human impacts. National Science Review, **7**, 132, **2019**.
9. HAO S., LI F. Water sources for typical desert vegetation in the Ebinur Lake basin. Journal of Geographical Sciences, **32**, 1103, **2022**.
10. LIN Y., MU G., XU L., ZHAO X. Grain size characteristics of the sand silt layers in the ancient delta of the dried Lop Nur lake (east Tarim Basin) and their environmental implications. Arabian Journal of Geosciences, **14**. **2021**.
11. DARVISHI BOLOORANI A., NAJAFI M.S., SOLEIMANI M., PAPI R., TORABI O. Influence of Hamoun Lakes' dry conditions on dust emission and radiative forcing over Sistan plain, Iran. Atmospheric Research, **272**, **2022**.
12. EBRAHIMI-KHUSFI Z., NAFARZADEGAN A.R., EBRAHIMI-KHUSFI M., ZANDIFAR S. Monitoring the water surface of wetlands in Iran and their relationship with air pollution in nearby cities. Environ Monit Assess, **194**, 488, **2022**.
13. MENENDEZ-SERRA M., ONTIVEROS V.J., TRIADO-MARGARIT X., ALONSO D., CASAMAYOR E.O. Dynamics and ecological distributions of the Archaea microbiome from inland saline lakes (Monegros Desert, Spain). FEMS Microbiol Ecol, **96**, **2020**.
14. GOLDSTEIN H.L., BREIT G.N., REYNOLDS R.L. Controls on the chemical composition of saline surface crusts and emitted dust from a wet playa in the Mojave Desert (USA). Journal of Arid Environments, **140**, 50, **2017**.
15. SWEENEY M.R., ZLOTNIK V.A., JOECKEL R.M., STOUT J.E. Geomorphic and hydrologic controls of dust emissions during drought from Yellow Lake playa, West Texas, USA. Journal of Arid Environments, **133**, 37, **2016**.
16. WANG Z., LI G., WANG X., GOU S., DENG Y., TAO S., ZHANG Y., YANG H., ZHAO W., JIN M. The Elements and Color of Lacustrine Record Revealed Lake Environmental Changes in Semiarid Northern China: A Case Study From Chagan Nur Lake of Southern Mongolian Plateau. Frontiers in Earth Science, **9**, **2021**.
17. MASHAT A.W.S., AWAD A.M., ALAMOUDI A.O., ASSIRI M.E. Monthly and seasonal variability of dust events over northern Saudi Arabia. International Journal of Climatology, **40**, 1607, **2019**.
18. VARGA G., ÚJVÁRI G., KOVÁCS J. Spatiotemporal patterns of Saharan dust outbreaks in the Mediterranean Basin. Aeolian Research, **15**, 151. **2014**.
19. FRIE A.L., DINGLE J.H., YING S.C., BAHREINI R. The Effect of a Receding Saline Lake (The Salton Sea) on Airborne Particulate Matter Composition. Environ Sci Technol, **51**, 8283, **2017**.
20. MOTAGHI F.A., HAMZEHPOUR N., ABASIYAN S.M.A., RAHMATI M. The wind erodibility in the newly emerged surfaces of Urmia Playa Lake and adjacent agricultural lands and its determining factors. Catena, **194**, **2020**.
21. YU H., ZHANG Z., WANG Z. Particle size characteristics of dry lake basin sediments in the southeastern Alashan Plateau. Journal of desert research, **41** (4), 177, **2021**.
22. LIU B., QU J., NING D., GAO Y., ZU R., AN Z. Grain-size study of aeolian sediments found east of Kumtagh Desert. Aeolian Research, **13**, 1, **2014**.
23. ZHANG Z., DONG Z. Grain size characteristics in the Hexi Corridor Desert. Aeolian Research, **18**, 55, **2015**.

24. ZHOU N., LI Q., ZHANG C., HUANG C., WU Y., ZHU B., CEN S., HUANG X. Grain size characteristics of aeolian sands and their implications for the aeolian dynamics of dunefields within a river valley on the southern Tibet Plateau: A case study from the Yarlung Zangbo river valley. Catena, **196**, **2021**.
25. FIELLER N.R.J., FLENLEY E.C., OLBRICHT W. Statistics of Particle Size Data. Journal of the Royal Statistical Society: Series C (Applied Statistics), **41**, 127, **1992**.
26. ZHANG Z., DONG Z., LI J. Grain-size characteristics of dune networks in china's tengger desert. Geografiska Annaler: Series A, Physical Geography, **97**, 681, **2016**.
27. CHENG H., HE J., ZOU X., LI J., LIU C., LIU B., ZHANG C., WU Y., KANG L., DEY S. Characteristics of particle size for creeping and saltating sand grains in aeolian transport. Sedimentology, **62**, 1497, **2015**.
28. MAHIQUES M.M.D., GOYA S.C.Y., MATOS M.C.D.S.N.D., OLIVEIRA R.A.U.D., KIM B.S.M., FERREIRA P.A.D.L., FIGUERIA R.C.L., BICEGO M.C. Grain-size end-members and environmentally sensitive grain-size components: A comparative study in the mud shelf depocenters off southern Brazil. International Journal of Sediment Research, **36**, 317, **2021**.
29. TU L., ZHOU X., CHENG W., LIU X., YANG W., WANG Y. Holocene East Asian winter monsoon changes reconstructed by sensitive grain size of sediments from Chinese coastal seas: A review. Quaternary International, **440**, 82, **2016**.
30. SHI Y., LIU Z., GAO J., YANG Y., WANG Y. The response of sedimentary record to catchment changes induced by human activities in the western intertidal flat of Yalu River Estuary, China. Acta Oceanologica Sinica, **36**, 54, **2017**.
31. GUAN Q., ZHANG J., WANG L., PAN B., GUI H., ZHANG C. Discussion of the relationship between dustfall grain size and the desert border, taking the southern border of the Tengger Desert and the southern dust deposit area as an example. Palaeogeography, Palaeoclimatology, Palaeoecology, **386**, 1, **2013**.
32. WANG Y., WU Y., LU R., PAN M. Application of Empirical Orthogonal Function (EOF) method to detect the spatial grain-size fractionation of aeolian sediment and comparison with other methods in case studies from northwestern China. Physical Geography, **39**, 216, **2017**.
33. CHUN X., ZHANG M.J., LIU M.P. The Coincident Relationships between the Qehan Lake Area Fluctuation and the Climate Change in the Nearly 40 Years. Applied Mechanics and Materials, **137**, 286, **2011**.
34. WENTWORTH C.K. A Scale of Grade and Class Terms for Clastic Sediments. The journal of geology, **30**, 377, **1922**.
35. FOLK R.L., WARD W.C. Brazos River bar [Texas]; a study in the significance of grain size parameters. Journal of Sedimentary Research, **27**, 3, **1957**.
36. WILLIAMS A.J., PAGLIAI M., STOOPS G. Physical and Biological Surface Crusts and Seals, Interpretation of Micromorphological Features of Soils and Regoliths, 539, **2018**.
37. MA Q., FEHMI J.S., ZHANG D., FAN B., CHEN F. Changes in wind erosion over a 25-year restoration chronosequence on the south edge of the Tengger Desert, China: implications for preventing desertification. Environ Monit Assess, **189**, 463, **2017**.
38. FU G., XU X., QIU X., XU G., SHANG W., YANG X., ZHAO P., CHAI C., HU X., ZHANG Y., WANG Q., ZHAO C. Wind tunnel study of the effect of planting Haloxylon ammodendron on aeolian sediment transport. Biosystems Engineering, **208**, 234, **2021**.
39. MAYAUD J., WEBB N., Vegetation in Drylands: Effects on Wind Flow and Aeolian Sediment Transport. Land, **6**, **2017**.
40. PYE K., Aeolian dust and dust deposits. Elsevier. **2015**.
41. PYE K., TSOAR H., Aeolian sand and sand dunes. Springer Science & Business Media. **2008**.
42. YONG GAO, Y.D., JI WANG, ZHONGJU MENG, XIAORUI SUN, CHAO ZHANG, YAJUAN WEI Variation in particle size of sediment on the surface of sand dunes with different plant scrubs and their sand fixation capacity. Transactions of the Chinese Society of Agricultural Engineering, **33**, **2017**.
43. WU Z. The sand and the geomorphology. Science Press. **1987**.
44. TSOAR H., PYE K. Dust transport and the question of desert loess formation. Sedimentology, **34**, 139, **1987**.
45. ZHANG Z., DONG Z., LI J., QIAN G., JIANG C. Implications of surface properties for dust emission from gravel deserts (gobis) in the Hexi Corridor. Geoderma, **268**, 69, **2016**.
46. ZHANG Z., LIANG A., ZHANG C., DONG Z. Gobi deposits play a significant role as sand sources for dunes in the Badain Jaran Desert, Northwest China. Catena, **206**, **2021**.
47. WANG X., CAI D., ZHU B., LOU J., LI D., ZHANG C.,CHEN S.,XU Y., CAI W., SU L., CHE H. Dust-sized fractions from dustfall and physical weathering in the Gobi Desert. Aeolian Research, **43**, **2020**.
48. ALKHAYER M., EGHBAL M.K., HAMZEHPOUR N. Geomorphic surfaces of eastern lake Urmia Playa and their influence on dust storms. Journal of Applied Sciences and Environmental Management, **23**, **2019**.
49. LYU Y., SHI P., HAN G., LIU L., GUO L., HU X., ZHANG G. Desertification Control Practices in China. Sustainability, **12**, **2020**.
50. DAI Y., DONG Z., LI H., HE Y., LI J., GUO J. Effects of checkerboard barriers on the distribution of aeolian sandy soil particles and soil organic carbon. Geomorphology, **338**, 79, **2019**.